Numerical study on the aerodynamics of an iced airfoil with scale-resolving simulations

Man-Long Wong , Aditya Ghate, Gerrit-Daniel Stich, Gaetan Kenway, and Cetin Kiris

Computational Aerosciences Branch
NASA Ames Research Center

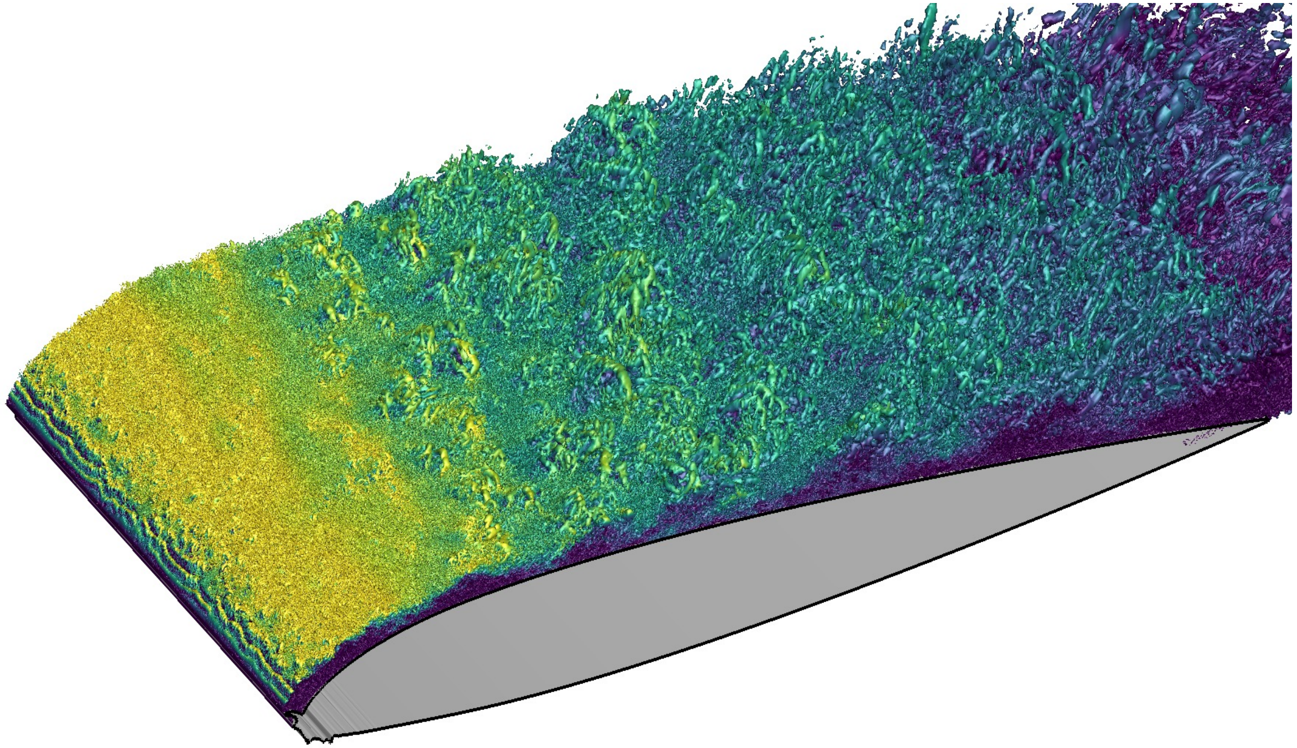

2023 AIAA SciTech Forum - 23–27 January 2023

Scope of This Work

- The performance of an aircraft is largely degraded when aerodynamic devices are contaminated with ice
  - Reduction in the maximum lift coefficient $C_{l,max}$ and stall angle of attack
  - Increase in drag, leading to more fuel consumption and decreased maximum flight range
- As experimental studies are expensive to perform, numerical computations, especially scale-resolving simulations, may provide an alternative for predictions and understanding of iced aerodynamics
- The capabilities of the body-fitted scale-resolving simulations in conjunction with penalty immersed boundary method, namely the hybrid body-fitted (BF)/immersed boundary (IB) approach, on predicting iced aerodynamics are investigated
  - The effects of ice accretion on the body are imposed on the flow using penalty / source terms added to the governing equations
  - The boundary treatments of the clean surface not covered by ice are handled with the more mature hybrid RANS/LES or wall-modeled LES (WMLES) turbulence approaches using body-fitted meshes
  - Improved ZDES mode 2 with enhanced protection and implicit time stepping used for the hybrid RANS/LES
  - Algebraic wall model and explicit time stepping used for WMLES
- The benchmark case of an airfoil NACA23012 with an artificial horn ice at the leading edge, **EG1164**, chosen to test numerical approaches at a subscale Reynolds number
  - $Re = 1.8\times10^6$; $M = 0.18$
  - Periodic extrusion of a 2D ice shape in the spanwise direction

Overset Curvilinear (Body-Fitted) Meshes

- Two different overset curvilinear meshes are designed for the WMLES
  - A baseline mesh and an improved mesh with refinement (colored in magenta) near the leading edge and the horn ice
- One overset curvilinear mesh used for the hybrid RANS/LES

$\Delta y^+ = 1$ is required for hybrid RANS/LES, compared to highly isotropic cells for WMLES

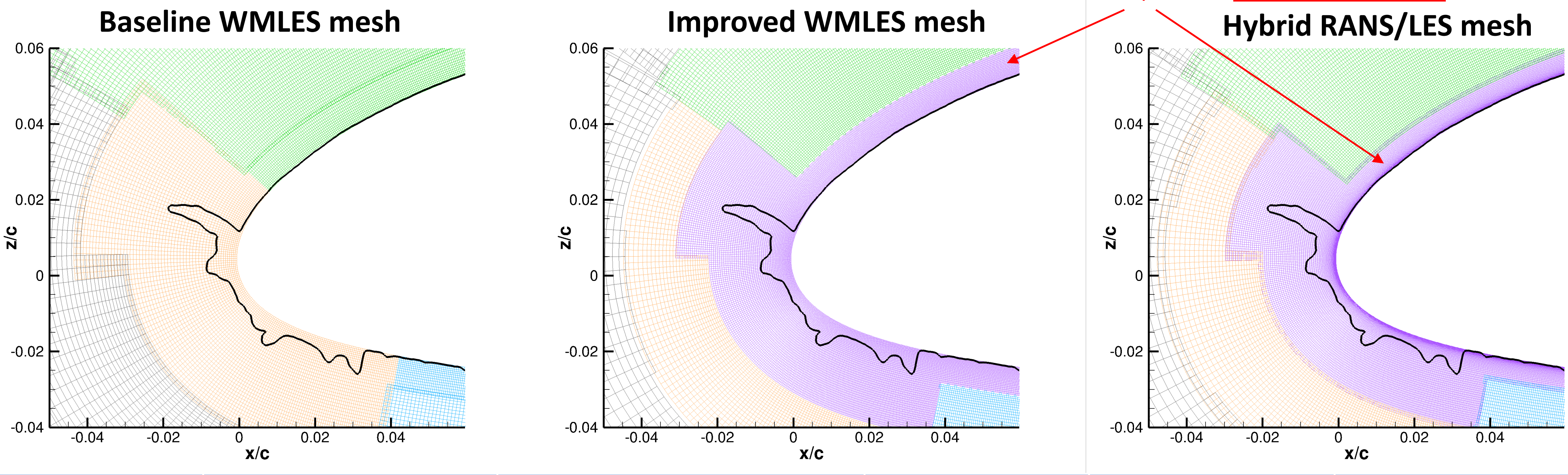

Grid	Min. wall normal grid spacing (× 10−3 c)	Min. grid spacing in other directions (× 10−3 c)	Number of grid cells (million)	Time step size (× 10−5 CTU)	Time scale of IB (× 10−5 CTU)
Hybrid RANS/LES	0.014	0.243	**367.7**	**24.94**	**0.14**
WMLES-baseline	0.486	0.486	**119.1**	**~ 3.82**	**4.09**
WMLES-improved	0.243	0.243	**206.6**	**~ 1.91**	**2.04**

Q-criterion

- Simulations are conducted at 4 α: 6.2°, 8.0°, 9.0°, 10.0°
- The flow separation at the horn is successfully triggered using the penalty immersed boundary method with the two turbulence modeling approaches, forming shear layers
- Due to the Kelvin-Helmholtz instability (KHI) caused by the large velocity difference across the shear layers, there is roll-up of spanwise vortices at the shear layers, followed by laminar-to-turbulent transition
- The iso-surfaces from the two approaches are qualitatively very similar, showing similar capabilities for predicting the KHI at the shear layers

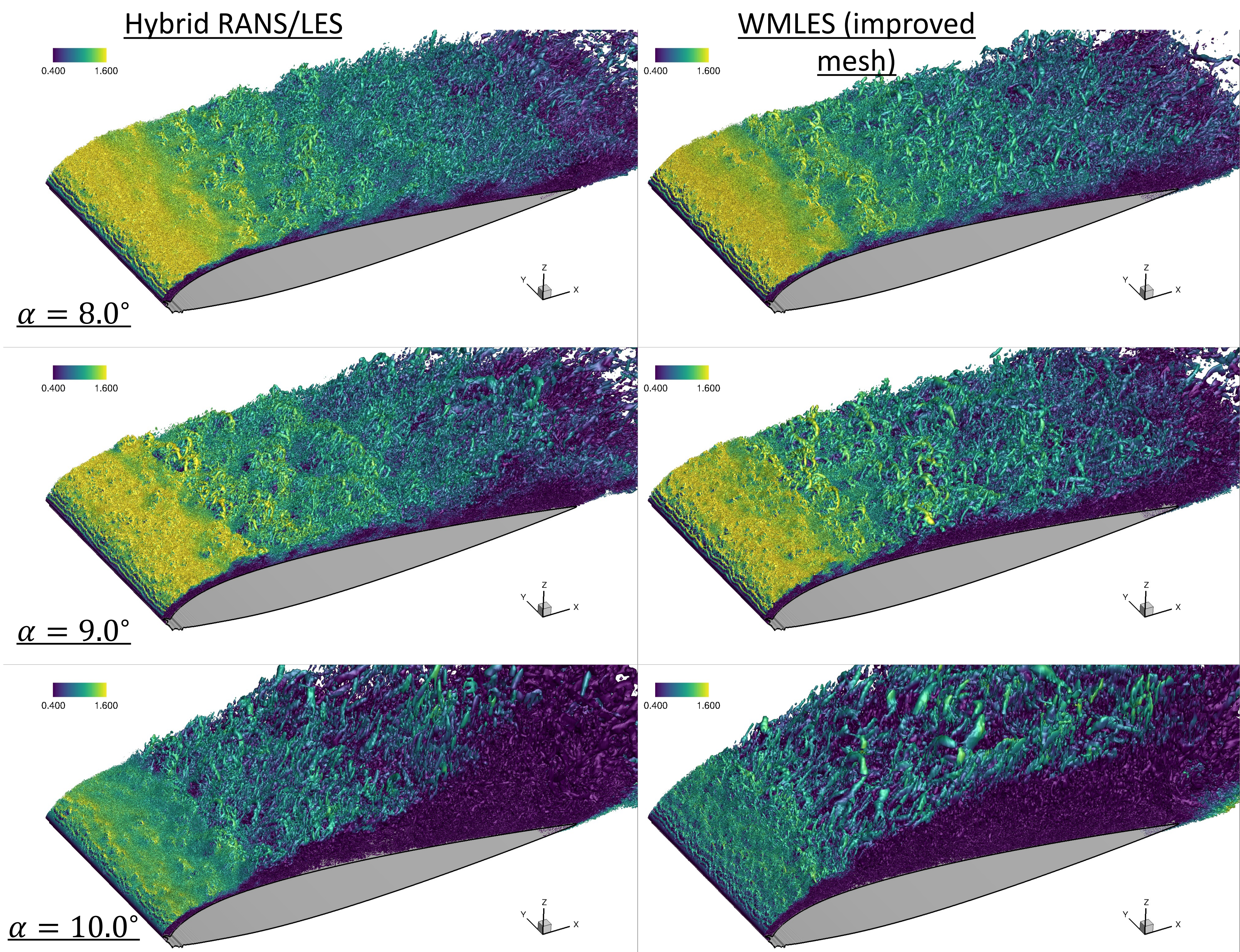

Mean Streamwise Velocity Component

- At the same α, the contours are similar between the hybrid RANS/LES and WMLES
- The magenta lines show the locations of flow separation and sizes of separation bubbles
- Flow separation can be seen at various corners formed by the ice accretion near the leading edge
- Hybrid RANS/LES predicts larger separation bubbles on the upper surface at higher α values
- At $\alpha = 10.0°$, both hybrid RANS/LES and WMLES results show separation starting from $x/c \approx 0.6$, indicating stall behavior

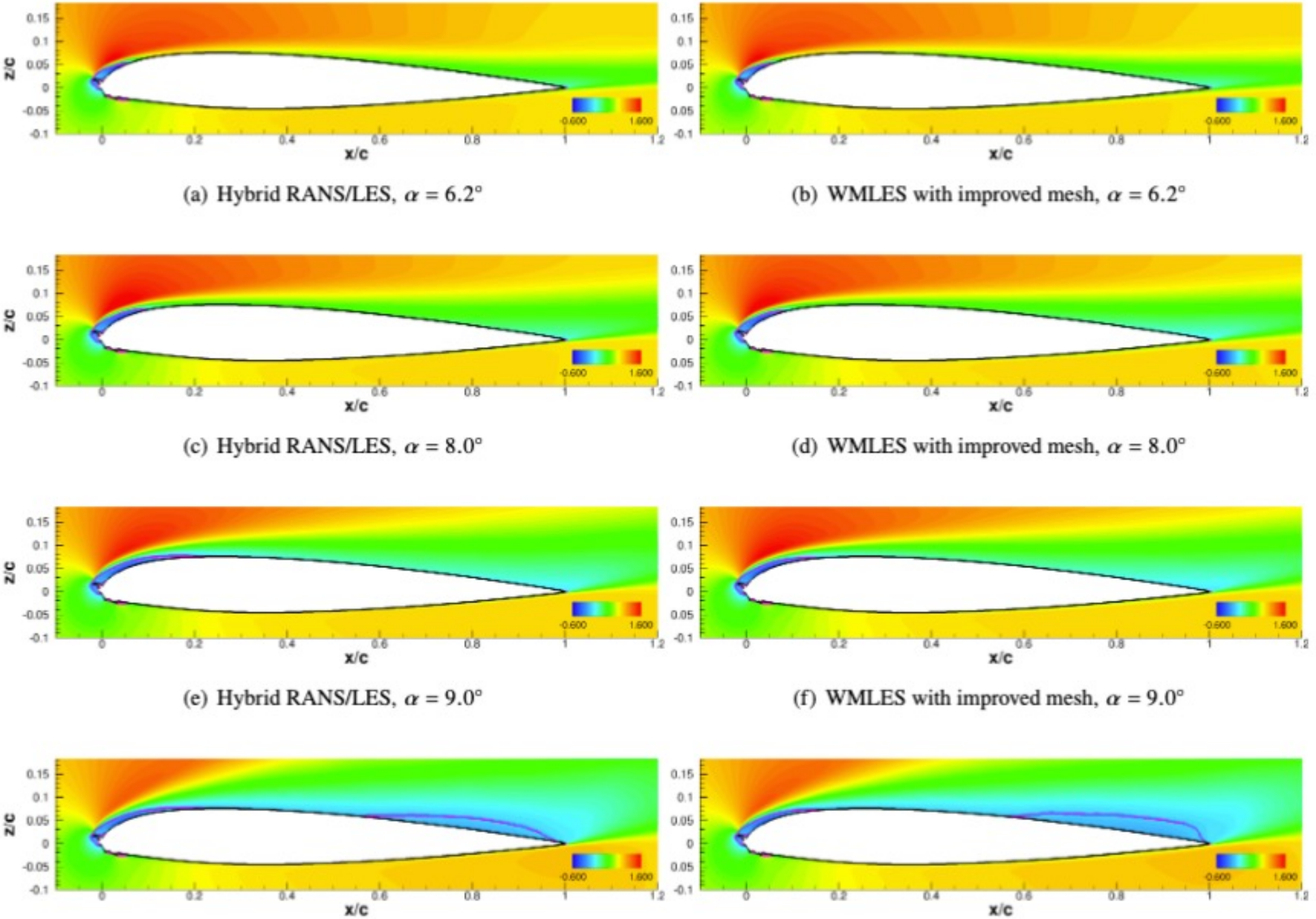

(a) Hybrid RANS/LES, α = 6.2°

(b) WMLES with improved mesh, α = 6.2°

(c) Hybrid RANS/LES, α = 8.0°

(d) WMLES with improved mesh, α = 8.0°

(e) Hybrid RANS/LES, α = 9.0°

(f) WMLES with improved mesh, α = 9.0°

(g) Hybrid RANS/LES, α = 10.0°

(h) WMLES with improved mesh, α = 10.0°

Aerodynamic loads and Pitching moments

- With ice accretion on the clean airfoil, the $C_{l,max}$ and the stall angle of attack decrease; the slope of C_m curve is more positive before stall; drag is also increased
- Except at $\alpha = 6.2°$, the unsteady RANS results has large under-prediction in the lift coefficients
- C_l from the scaling-resolving simulations agree much better with the subscale experimental results, such as at $\alpha = 8.0°$ and $\alpha = 9.0°$
- C_l from WMLES with the improved mesh is more accurate due to more accurate IB representation of the horn ice with finer grid resolution
- Larger RMS (represented by error bar) is seen in all aerodynamic coefficients at $\alpha = 9.0°$ for the hybrid RANS/LES
- C_m from WMLES seems to agree better with the subscale experimental results at $\alpha = 9.0°$
- Large number of convective time units (CTU), 100 CTUs, are required due to low frequency oscillations in the coefficients for $\alpha = 9.0°$ and $\alpha = 10.0°$

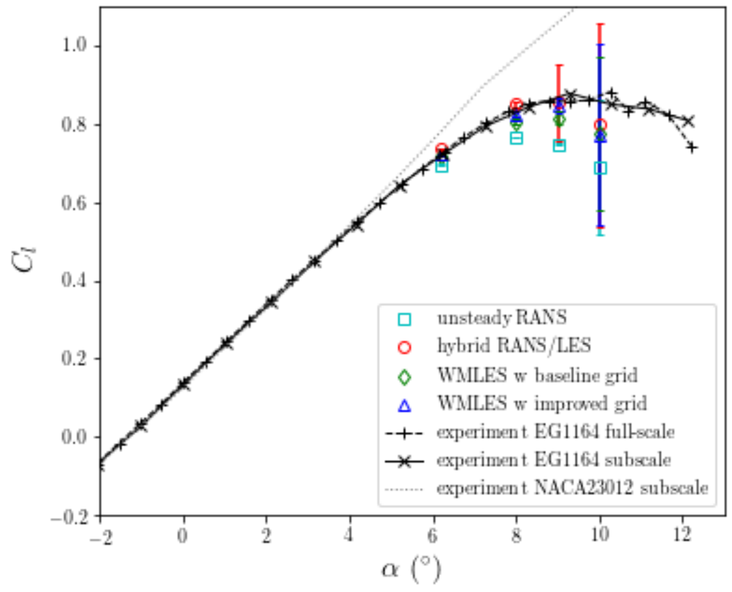

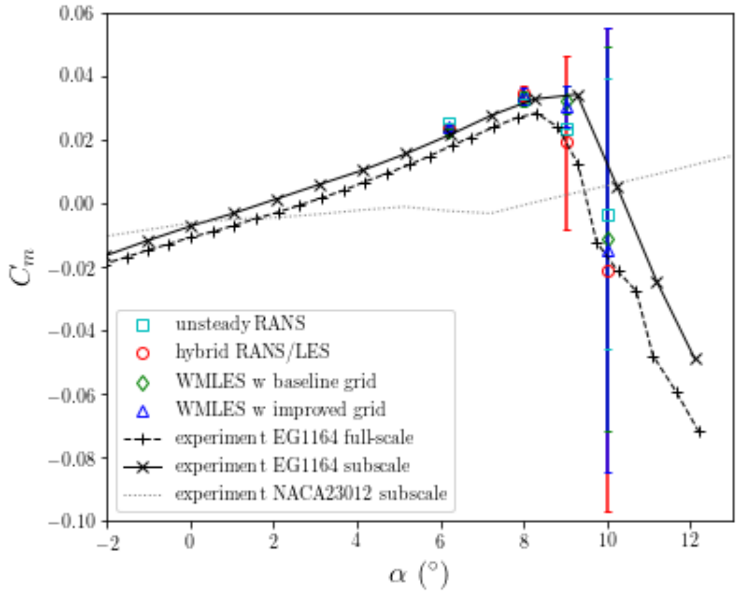

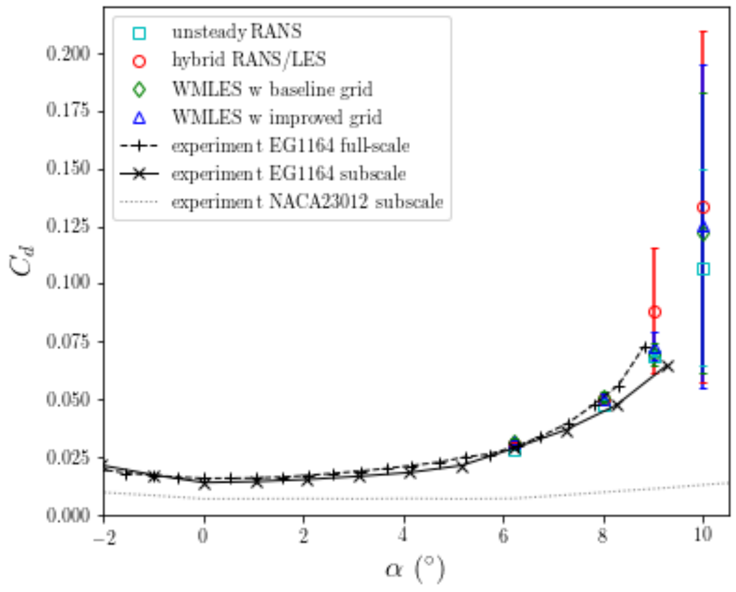

Pressure Coefficients

- The C_p distributions from both hybrid RANS/LES and WMLES (improved mesh) are almost identical at $\alpha = 6.2°$ and $\alpha = 8.0°$
- The negative plateaus caused by flow separation at the leading edge, and the pressure recovery inside the separation bubble are well captured at $\alpha = 6.2°$ and $\alpha = 8.0°$
- Larger differences are seen at $\alpha = 9.0°$ and $\alpha = 10.0°$. The hybrid RANS/LES has less negative pressure plateau on the suction side and hence it has a smaller pitching moment coefficient at $\alpha = 9.0°$

$\alpha = 6.2°$

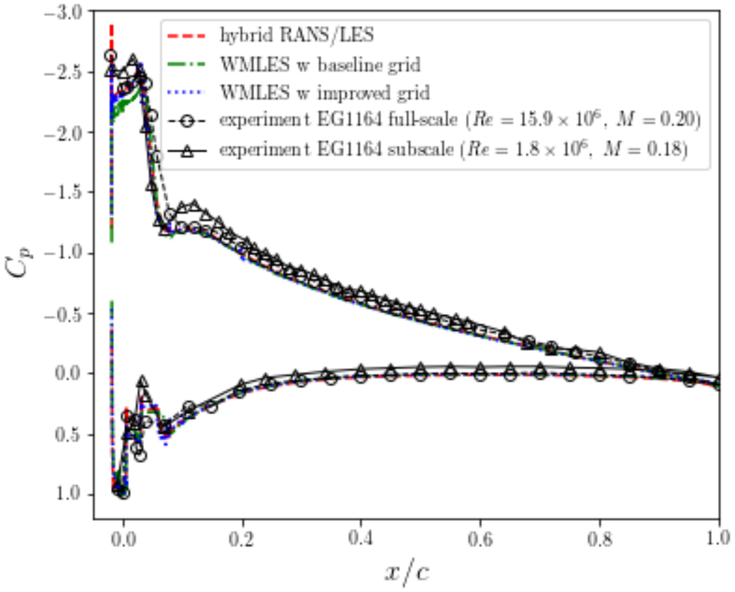

$\alpha = 8.0°$

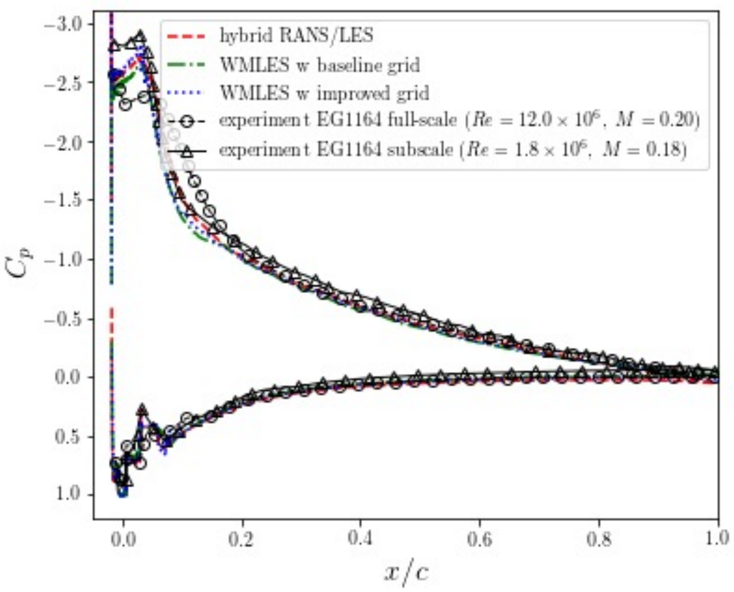

Different angles of attack of hybrid RANS/LES

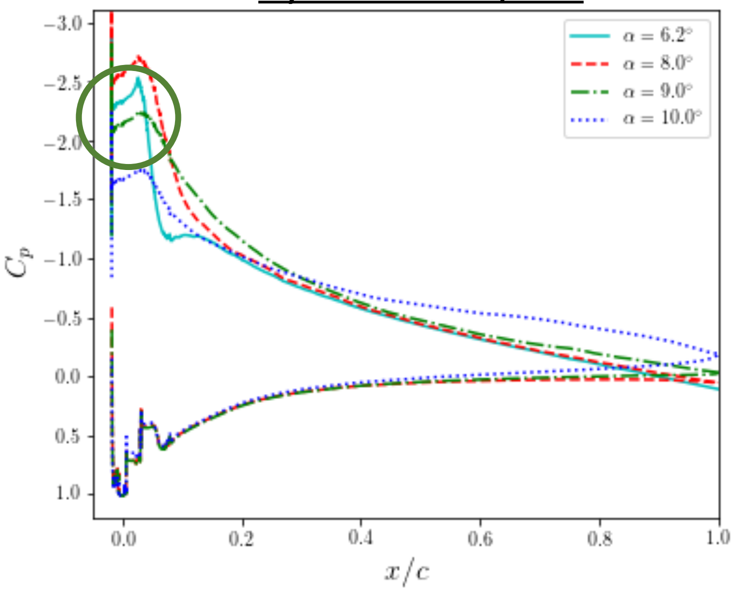

Different angles of attack of WMLES

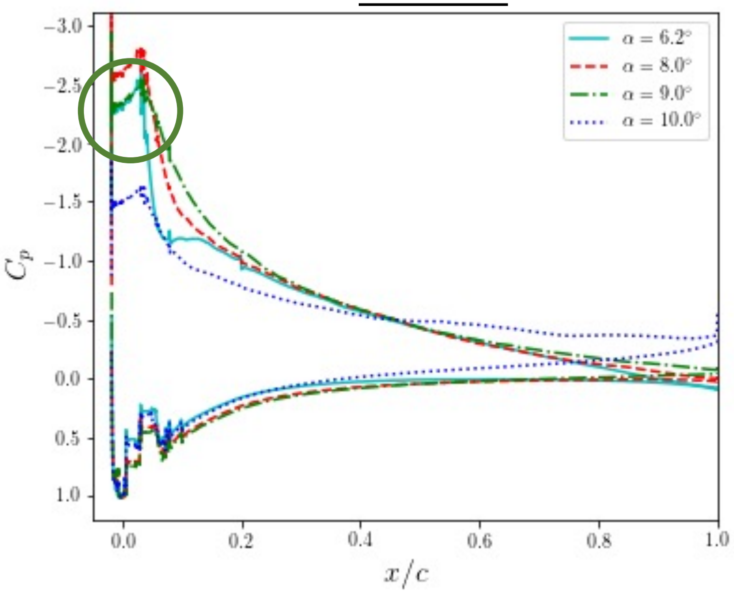

Turbulent Kinetic Energy (TKE)

- Peaks of TKE contours from different α are all at locations shortly downstream of the upper horn ice tip and the peak values are quite independent of the angle of attack
- These regions of highly turbulent flows are the results of the rapid transition to turbulence caused by the Kelvin-Helmholtz instability (KHI) at the shear layer induced from the horn ice tip
- As α increases, there is a wider spread of high TKE with larger thickness on the upper surface of the airfoil and and this indicates more turbulent flow induced by the horn ice

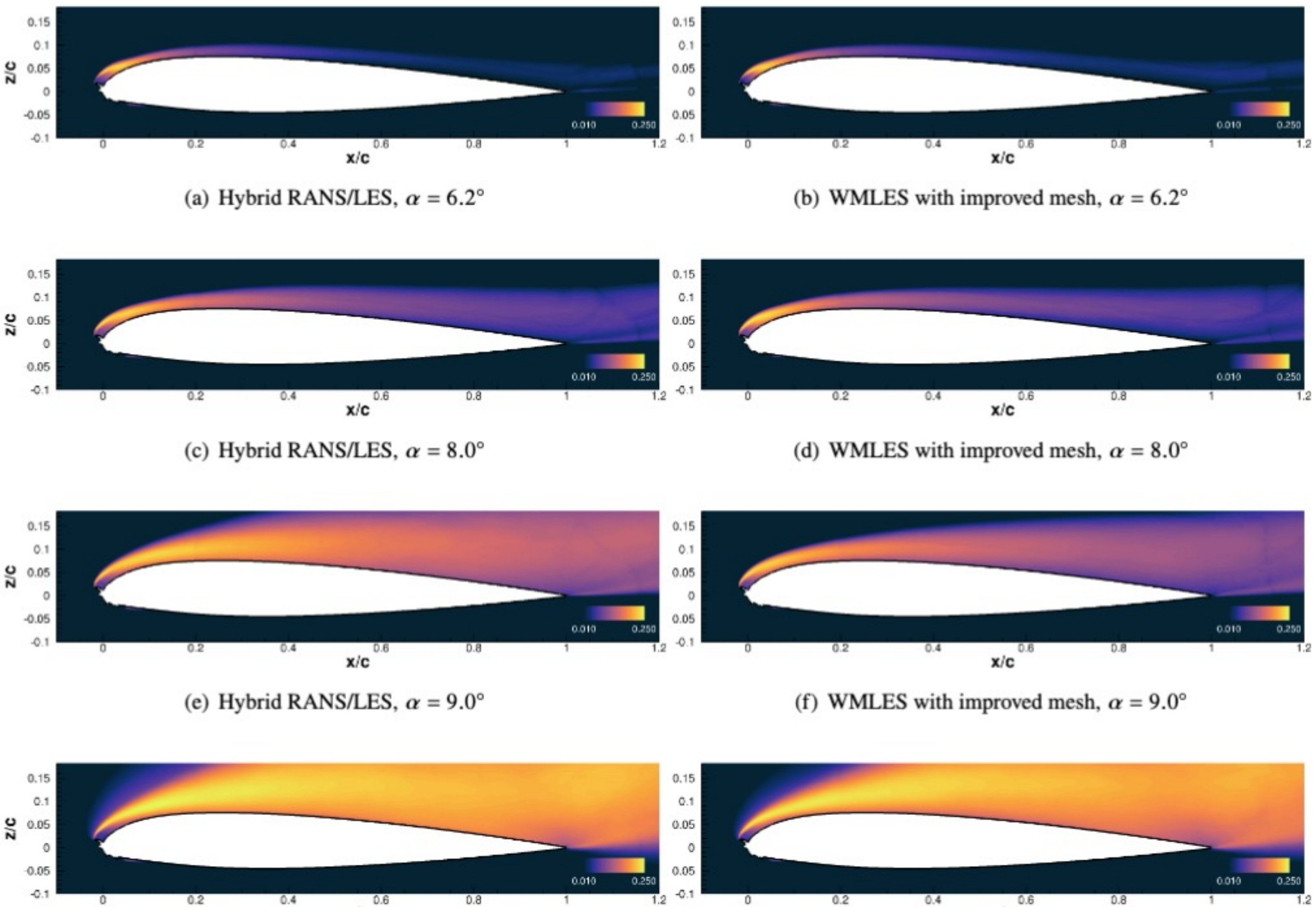

(a) Hybrid RANS/LES, $\alpha = 6.2°$

(b) WMLES with improved mesh, $\alpha = 6.2°$

(c) Hybrid RANS/LES, $\alpha = 8.0°$

(d) WMLES with improved mesh, $\alpha = 8.0°$

(e) Hybrid RANS/LES, $\alpha = 9.0°$

(f) WMLES with improved mesh, $\alpha = 9.0°$

(g) Hybrid RANS/LES, $\alpha = 10.0°$

(h) WMLES with improved mesh, $\alpha = 10.0°$

Spectral Proper Orthogonal Decomposition (SPOD)

- In order to identify any coherent structures of the flows around the iced airfoil that are caused by the unstable Kelvin-Helmholtz instability (KHI) modes in the shear layer, the SPOD data-driven method is used
- The spectral POD, or SPOD, is different from the "standard" POD as the former has a space-time decomposition with Fourier transform in time under the assumption that the flow data post-processed is statistically stationary
- As the spanwise direction is also homogenous, Fourier transform is applied in the spanwise direction. As a result, SPOD modes are computed at each combination of l-th frequency and m-th mode number in the spanwise direction
- The SPOD based on energy defined with the pressure and TKE norms are used
- Time-resolved volume data in a box around the leading edge of the iced airfoil is collected using WMLES with improved mesh
- 20 convective time units (CTUs) with 1000 snapshots per CTU at different α
- Peaks found at 5 Strouhal numbers for leading SPOD mode when the spanwise mode number is small: St =31.5, 48.3, 96.6, 147.1, and 195.9
- $St = 31.5$ corresponds to KHI at the lower horn ice. The St decreases with α
- $St = 48.3$ corresponds to fundamental Strouhal number of KHI at the upper horn ice; $St = 96.6$, 147.1, and 195.9 are the harmonics; The fundamental St remains unchanged with α

Real parts of SPOD eigenvectors at different α and $m = 0$ based on pressure norm

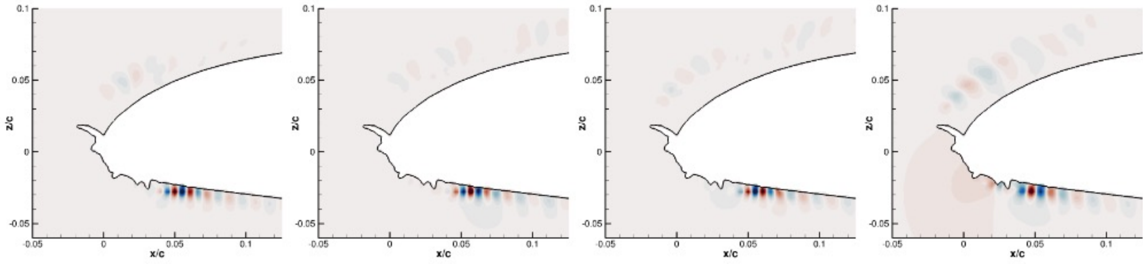

(a) $\alpha = 6.2°$ at $St = 36.2$ (b) $\alpha = 8.0°$ at $St = 31.5$ (c) $\alpha = 9.0°$ at $St = 31.0$ (d) $\alpha = 10.0°$ at $St = 27.3$

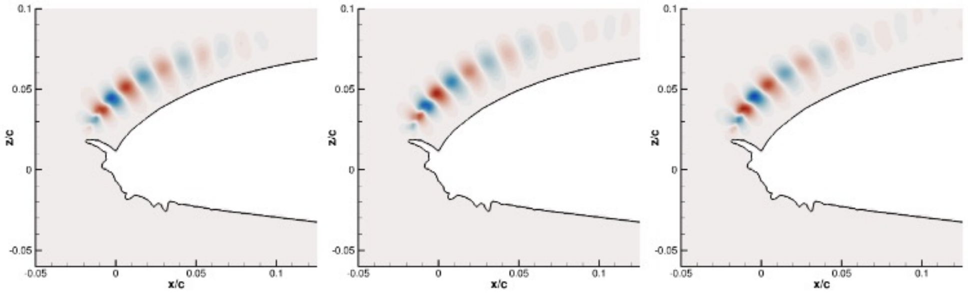

(a) $\alpha = 8.0°$ at $St = 48.3$ (b) $\alpha = 9.0°$ at $St = 47.8$ (c) $\alpha = 10.0°$ at $St = 48.3$

Peaks identified at 5 Strouhal numbers at $\alpha = 8.0°$

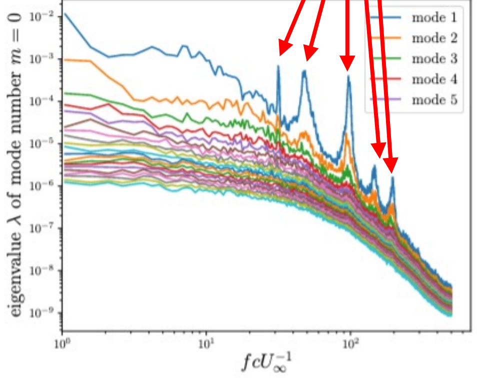

(a) Pressure norm

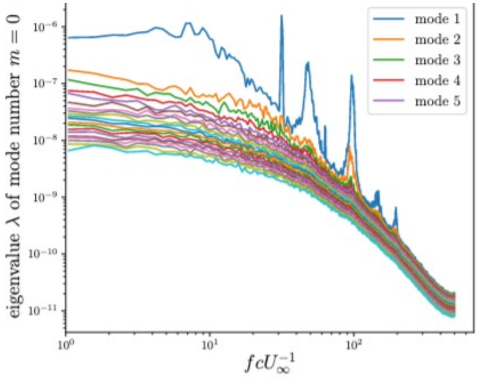

(b) TKE norm

Concluding Remarks

- When sufficient mesh resolution is used, results from hybrid RANS/LES and WMLES coupled with the penalty IB method have good comparison with the experimental results at low angles of attack and reasonably good predictions for α near and after stall

- These scaling-resolving simulation results outperform the unsteady RANS results in predicting $C_{l,max}$ and α_{stall}

- With the increase of the angle of attack, it was found that the region with high turbulence intensity induced by the unstable shear layer spreads quickly over the entire upper surface of the airfoil

- The coherent KHI modes at the upper and lower shear layers were successfully extracted using SPOD; these modes have large-scale variations in the spanwise direction and low-rank behavior

Acknowledgments

- This work was partially funded by the NASA's Aeronautics Research Mission Directorate's (ARMD) Transformational Tools and Technologies (Tˆ3) and the Advanced Air Transport Technology (AATT) projects
- NASA Advanced Supercomputing (NAS) facility at NASA Ames Research Center
- Jeffrey Housman, Oliver Browne, and other LAVA team members at NASA Ames Research Center for helpful discussions and advice
- Andy P. Broeren from NASA John H. Glenn Research Center for valuable discussions